Experiment of concrete pavements at LCPC's fatigue test track

J.-M. Balay (1)
B. Darbois (2)
J.-C. Gramsammer (1)
J.-L. Nissoux (1)
A. Sainton (3)

(1) LCPC : Laboratoire Central des Ponts et Chaussées, Ministry of Infrastructure, Housing, Transport, and Space, France
(2) SFIC : Syndicat Français de l'Industrie Cimentière
(3) SPECBEA : Syndicat Professionnel des Entrepreneurs de Chaussées en Béton et Equipements Annexes

1. OBJECTIVES OF THE EXPERIMENT

The standard for the design of concrete structures in France is the Catalogue des Structures de Chaussées Neuves (Design Guide of New Pavements Structures), a set of regulations issued in 1977 and updated in 1988 (1) that applies to all new structures.

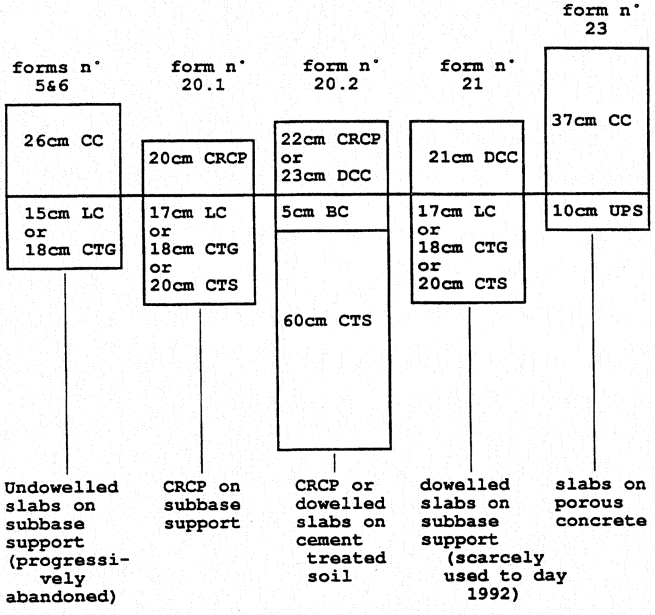


Figure 1 : French design guide of new pavements. Comparison of the 5 concrete structures, example.

Six sheets of it refer to concrete structures. Figure 1 shows the choices offered by this French catalogue. The example assumes high traffic T1 (4.5 to 11.2 millions of trucks for 20 years) and an average soil PF2 (Young modulus 50 MPa).

The french Highway Department and the concrete pavement Contracting and the lime and cement Industries, represented by their national associations, in 1991-1992 initiated a major experiment on the pavement fatigue test track of the Laboratoire Central des Ponts et Chaussées (LCPC), in order to check the soundness of the designs proposed by the Catalogue for concrete pavements.

The experiment began on February 1991. In to day (August 1992), one million loadings remain to be performed. They are expected to be completed at the end of December 1992. This article presents the tested structures and their instrumentation, the first observed damages, and the first results of measurement and of theoretical modelling of structures using finite element method.

2. THE LCPC'S TEST TRACK

The Road Structure Circular Test track was commissioned at the beginning of 1984 at the Nantes station of the Laboratoire Central des Ponts et Chaussées (2). From year to year, the working capacity of this facility has been increased through extensions or improvements to one or another of its sub-systems: machine, infrastructure, measurement unit (photo 1). Since its commissioning it has

simulated the passage of 36 millions trucks (about 35 times as many loadings as the AASHO tests) in the course of about sixty experiments.

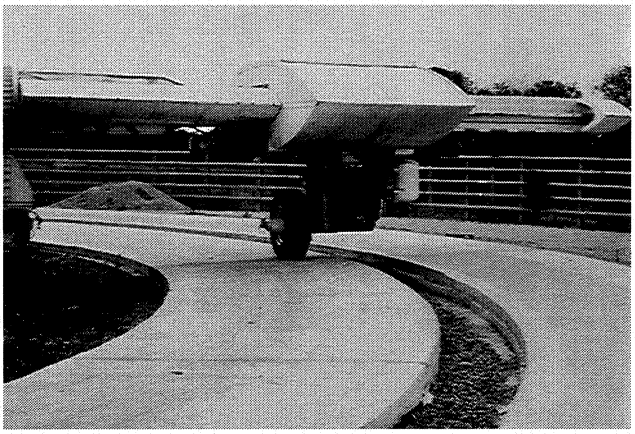


Photo 1. The LCPC's fatigue test track - General view (it is equiped here with large single wheels instead of twin wheels used for this experiment)

With its four arms 20 metres long, it is driven by a thousand horsepower electro-hydraulic engine at its centre, to speeds that may exceed 100 kph at the circumference. The test track simulates the passage of single axles having adjustable weights which may very between 9 and 15 tons at a rate that may exceed one million loadings a month.

It can also tow tandem axles and single wheels with large tyres. The force applied to the 6 m wide circular test pavements is kept constant by an original suspension system that uses an intermediate rolling support. The radii of rotation, like the transverse displacements of the wheel, can be adjusted while the test track is running.

The installation can be transported within a week from one of the three sites to another. Finally, it is a system that operates automatically practically 24 hours a day.

3. OVERALL ORGANIZATION OF TESTS, EXPERIMENTAL STRUCTURES

3.1 Experimental arrangements

For the tests on concrete pavements, the fatigue test track made it possible to test four different structures at a time on a single ring. Each structure is therefore a quarter of a ring long, making the length of the structures tested 25 or 30.5 meters according to the radius of the ring.

The experiment included two series of tests: on an inner ring having a mean radius of 15.50 meters (ring 1), and on an outer ring having a mean radius of 19.50 meters (ring 2). It was decided to test the same types of structures on both rings. The thickness of a given type of structure differs from one ring to the other, in order to withstand different numbers of passes of axles according to the ring. This brought the total number of different structures tested to eight, broken down into four types denoted A, B, C, and D.

3.2 Structures tested

The four structures were chosen from amongst the five structures in the catalogue. Continuously reinforced concrete pavement (CRCP) was set aside because of experimental difficulties and because the ability of small circular sections to represent this type of reinforced structure was doubted.

The catalogue structures tested on the circular track were:

- short slabs of concrete cement with no subbase (sheet 23), hereinafter referred to as structure A ;
- short slabs of lean concrete with no subbase. This is a variant of sheet 23, that the catalogue reserves for low traffics: structure B ;
- undowelled short slabs on treated subbase (sheets 5 and 6) : structure C ;
- dowelled short slabs on treated subbase (sheet 21) : structure D.

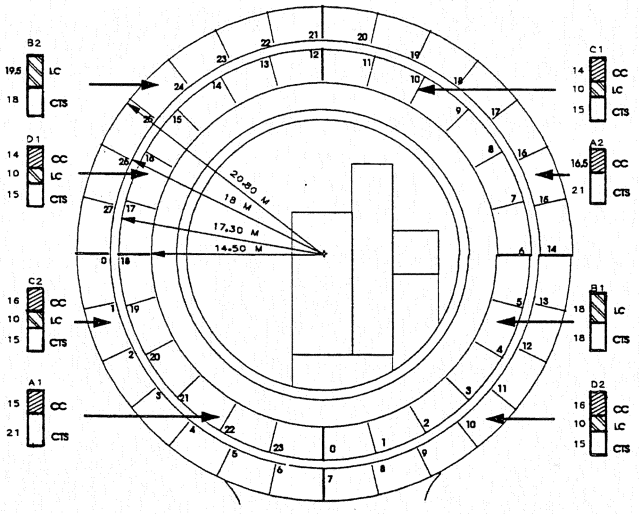


Figure 2 : Structures tested on the LCPC's test track : cross-sections and thickness, plan view and joints numbering

The thicknesses given to structures D and C on a given ring are the same. The design model in fact leads to a reduced thickness for structure D, with dowels. To allow direct comparisons of the behavior of undowelled structures C and dowelled structures D, this reduction of thickness was not applied to structure D for the tests on the circular track.

Stage 1 was a preliminary stage that included a limited number of axles repetitions, set at 1.1 million. It was conducted on inner ring 1, having an average radius of 15.50 meters, from January to April 1991. The structures are denoted A1, B1, C1 and D1.

Stage 2 constituted the main stage of testing. Structures A2, B2, C2 and D2 were designed for a total traffic loading of 3 million axles. They were placed on outer ring 2, which has a larger radius (19.40 m). Stage 2 was itself divided into two steps. The first step was from February to May 1992 and included 2 million loadings. The workload of the fatigue test track made it necessary to postpone until November 1992 the implementation of the second step, the end of which is expected at the end of December 1992.

The width given to the eight experimental sections is constant at 2.80 meters. Each structure of inner ring 1 has six slabs produced by the sawing of joints during construction. The mean length of each slab measured on the mean perimeter is 4.16 meters. On outer ring 2, each section has seven slabs and the mean length is 4.35 meters.

The plan view of the eight experimental sections on the two rings is shown on figure 2. It also indicates the numbering of the 52 joints between slabs, used below to identify the different slabs.

4. INSTRUMENTATION OF STRUCTURES, SURFACE MEASUREMENTS

4.1 Strain gauge equipment

The French pavement design method is called "rational". It is based primarily on the numerical determination of the stresses and deformations induced in the structures by a reference axle. The maximum tensile stresses, combined with the fatigue strength of the material (Wöhler's model) and with the load equivalency factors of the actual traffic, are used to determine the number of loading cycles the structure can stand and thus its life time. Determining the strains or stresses in the structures is therefore the basis of the French design method.

The semi-infinite multi-layer two-dimensional models used for asphaltic pavements (ref.4) are ill suited to concrete structures. These rigid structures necessarily require a more complex 3-dimensional model. It must be able to reproduce the effects of temperature gradients in the structures. The finite-element calculation method (fem) can help in dealing with this complex problem. But the application of the fem to concrete pavements is recent, and at the moment there is rather little experimental data for the validation and fitting of this model. This explains the number of strain gauges placed in the structures tested on the circular track. There were 190 strain gauges embedded in the concrete, in the subbases, or glued to the dowels for the tests on ring 1, and there are 200 for ring 2.

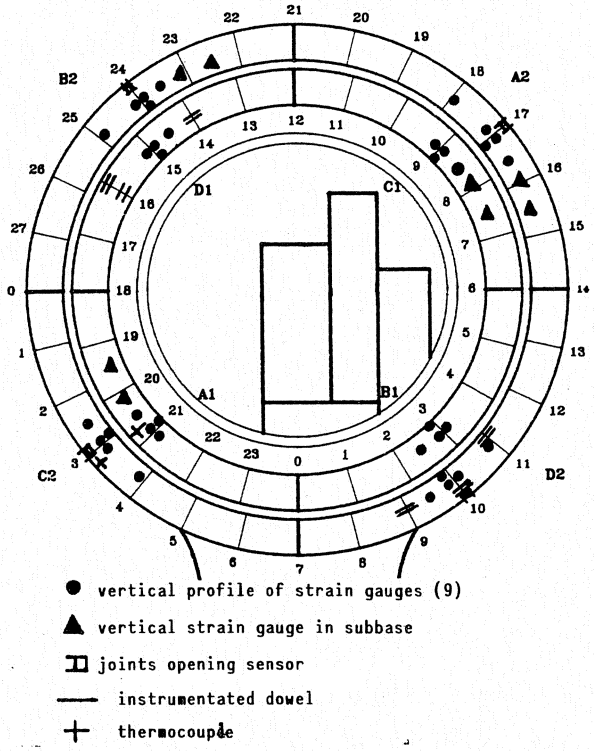


Figure 3 : Positionning of the strain gauges and measuring equipments in the structure

Figure 3 shows the principles of the positionning of these strain gauges in the structures. A primary slab is chosen for strain gauge measurements on each of them. In the concrete slabs, horizontal strains are measured at three levels: 2 cm from the top surface, at mid-height, and 2 cm from the bottom surface. At each of these measurement points, three strain gauges are placed in a horizontal rosette, in the longitudinal direction, transverse direction and diagonal direction. Each

vertical profile of strain gauge measurements in the concrete therefore includes nine strain gauges, making it possible to determine the principal horizontal stresses at three levels.

Each of the four structures contains five profiles of this type. As shown on figure 3, they are located at the center of the measurement slab in the centerline of the wheel path, on the upstream and downstream sides of the next joint, on the upstream side of the far joint of the next slab; and at the upstream corner of the measurement slab. Strain gauges are also placed vertically at the top of the cement-treated sand subbase and at the top of the soil, on structures A1, C1, A2, and B2 only.

4.2 Surface measurements

The monitoring of traffic-induced strains by strain gauges is accompanied by surface measurements, which serve to monitor changes in the surface movements of the slabs under loads. The measuring devices are shown in figure 4.

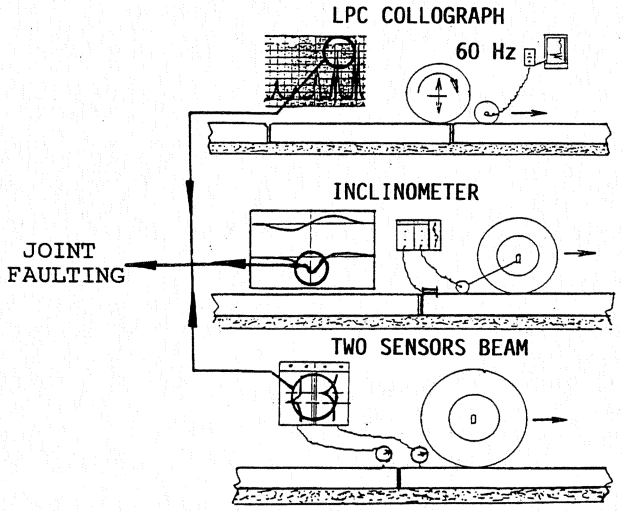


Figure 4 : Devices for surface measurement on LCPC's test track.

For slow speeds (2 kph), two measuring systems are used. One is a two-sensor beam to record joint faulting. It uses two potentiometer displacement sensors having their plungers in contact with the corners of the slabs on either side of joints and cracks. The sensor housings are mounted on an immobile reference beam supported from the slab.

The other is the inclinometer. This very sensitive device delivers a voltage proportional to the inclination of the structure on which it rests. The measurements are made in the centerline of the load used for these tests on the circular track, i.e. in the gap between wheels of a pair.

For high-speed measurements, seismic sensors (geophone) glued to either side of the joints are used.

A final type of surface measurement is made using the LPC collograph (5). This device consists of a 60 Hz vibrating mass rolling on the pavement. A sensor, also rolling (hydrophonic wheel), travels 30 cm ahead of the vibrating mass that constitutes the excitation. It delivers a continuous signal proportional to the amplitude of the vertical vibration of the pavement surface.

4.3 Other measurements

On structure A1 and C2, figure 3 also shows the 7 temperature sensors used to record the temperatures in the structures and at various levels in their subbases.

On each ring, six dowels distributed along two transverse joints of structure C also have strain gauges glued to the steel itself (figure 5a).

Two longitudinal strain gauges are glued to the top and bottom fibers: they provide information about bending forces. Two diagonal gauges glued to the dowels at mid-height provide information about shearing forces.

For the tests on the second ring, displacement sensors are also installed (figure 5b). They can be used for continuous measurement of the horizontal opening of the downstream joints of the main measurement slabs of A2, B2, C2, and D2.

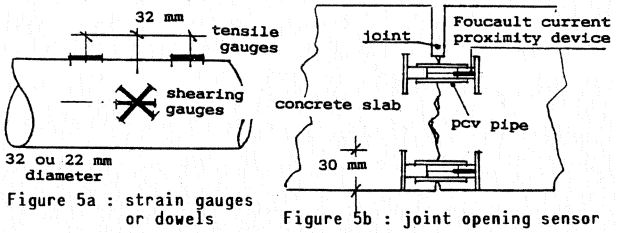


Figure 5a : strain gauges or dowels

Figure 5b : joint opening sensor

Figure 5 : Complementary measuring devices for stresses in dowels and openings of joints

5. LOADING CONDITIONS, TRAFFIC

The nominal load chosen for the tests was the single half-axle with twin wheels (32.5 kN per wheel). This is the reference load of the French design method. The end of each of the four arms of the fatigue

tester is fitted with such a 65 kN pair of wheels.

In normal operation, the radii of rotation of the four half-axles are adjusted to 15.5 m on ring 1, and to 19 m on ring 2.

6. CONSTRUCTION OF THE EXPERIMENTAL STRUCTURES

The experimental pavements were built by the contractors of the Syndicat Professionnel des Entrepreneurs de Chaussées en Béton et Equipements Annexes (SPECBEA), under the supervision of the Gailledrat Construction Company and the LCPC.

Inner ring 1 was built in cold weather: from the beginning of December 1990 to mid-January 1991. The cement-treated sand and lean concrete subbases of structures C2 and D2 were built at the same time. The rest of the construction of outer ring 2 was done in warmer weather: from mid-August to mid-September 1991.

The earthworks were made by adding approximately 10 cm of clayey sand identical to the soil in place at the circular test track site. Levelling was done by hand because of the small size of the track. Compaction was done with the small vibrating roller on structures A1, B1, C1, D1, C2, and D2 (winter 1990). A heavier compactor was used for structures A2 and B2 (summer 1991).

The large clay content of the soil and the high level of water table lead to rather low properties for the soil platform on the site of the test track: about 5 for CBR index, and Young modulus between 30 and 50 MPa.

The subgrade is of sand treated with 3.5 % cement. It was levelled by hand and compacted by the same plant as the soil.

On structures A1, B1, C1, D1, C2, and D2, built in cold weather (temperatures sometimes below 0°C at night), the setting and hardening of the cement-bound sand were especially slow. On these structures, the surface of the subgrade was even locally damaged by site traffic before the pouring of the concrete.

The subbase lean concrete (structures C and D) was placed by a slipform paver. This same machine was used to cast the concrete of the slabs on the eight structures.

The view of photo 2 shows the concrete plant of structure D1. The instrumentation of joint 16 can be seen in the foreground.

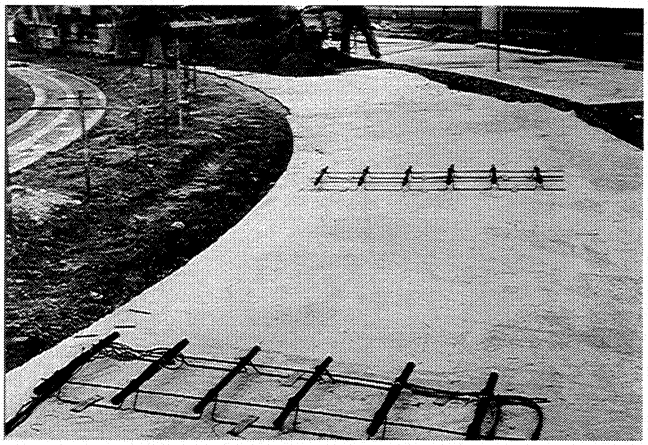


Photo 2 : Concrete plant of structure D1 (the insrumented dowels of joint 16 are seen in the foreground)

All dowels were the same length : 60 cm. On the first ring, the dowels used in structure D1 are 32 mm in diameter, for a thickness of concrete of 14 cm. Six dowels are instrumented. Their section is in fact oversize with respect to normal French site practice.

On the second ring, only joint 13 is equipped with six dowels 32 mm in diameter, two of which are instrumented. The other six joints are equipped with dowels 22 mm in diameter, four of which are instrumented. These arrangements are intended to allow comparison of the behavior of dowels of different diameters.

Formulation kg/m3	Subbase concrete	Pavement concrete
0/3 washed sea sand	770	655
6/10 crushed gravel	465	480
10/14 crushed gravel	350	365
14/20 crushed stones	385	365
CPJ 55 cement	140	300
Fly ash	40	
Filler	40	30
Plasticizer	0.77	1.15
Air entraining agent	0.22	0.44
Water	150	160
Slump (cm)	3	3.5
Air content (%)	4.7	5.6
Mecanical properties (MPa)	**Subbase concrete**	**Pavement concrete**
Site tests-bending tensile strengh (7 days)	1.3	2.7
Site tests-bending tensile strengh (28 days)	1.7	3.15
Site tests-compressive strengh (28 days)	14.2	34
Young's modulus	20 240	27 530

Table 1 : Formulation (kg/cu.m) and mechanical properties (MPa) of cement concretes

The formulas and mechanical characteristics of the concretes used are given in table 1.

A better quality and greater homogeneity are obtained with structures A2 and B2, which were made in hot weather and also have denser subbases. This is established by various checks made: levelling of the different layers, mechanical characteristics of the cement-treated sand and of the concretes.

7. OPENING OF JOINTS : RESAWING

Following the technique in usage at French sites, the joints are sawn approximately 24 hours after the concrete is poured. They are sawn by a power saw in the upper quarter of the thickness of the slabs, as shown by the drawing of figure 2 and 5b.

A month after the pouring of the concrete, it was confirmed visually that almost all of the joints of the different structures were in fact open. However, the whole joints of structures A1 and B1, and the joint 9 of C1, exceptions. The continuity at joints of these structures was still detected at 0.5 million loadings.

Structures A and B have a draining carpet interposed at the interface between the cement-treated sand and the concrete. The low temperatures during the pouring of structures A1 and B1, together with the presence of the draining carpet, explain the failure to open of the joints of these structures. It was decided after 0.5 million loadings (March 1991) to perform forced opening of the joints on structures A1 and B1. They were opened by repeated power sawing through the whole thickness of the concrete slabs.

Likewise, the joint 9 of structure C1, not open, had been sawn through its whole thickness at 250,000 loadings.

8. PROGRAM OF ROTATIONS AND MEASUREMENTS

The first rotations of the fatigue test track on ring 1 began on 18 February 1991. The test ended on 15 April 1991, after 1.1 million loadings. On ring 2, the rotations started on 23 January 1992. The first stage of this second series of tests ended on 22 May 1992, after 2 million loadings. As of today (August 1992), 1 million loadings remain to be performed. The tests will be resumed in November 1992.

The speed of rotation in normal operation is 10 revolutions per minute, corresponding to a linear axle speed of 58.4 kph on ring 1 and 73.1 kph on ring 2. For the duration of some measurements on the strain or surface gauges, the speed of rotation can however be reduced to 0.3, 0.5, or 1 rpm.

The interval between measurements was approximately 250,000 loadings on ring 1 and approximately 350,000 loadings for the first stage of testing on ring 2. In addition, there were visual observations of the surface of the structures and damage surveys at intervals ranging from 50,000 to 100,000 loadings.

The ordinary series of measurements are used to track changes of the strains in the structures with the number of loadings (strain gauge measurements) and movements of the slabs under the effect of tyres (surface measurements).

Special series of measurements (strain gauges) are used to monitor the behavior of the structures during a daily temperature cycle. Other special series are used to evaluate the effects on the gauge measurements of the speed of the axles, or the effects of the position of the axles with respect to the gauges (research of maximum tensile strains).

9. OBSERVED DAMAGE AND SURFACE MEASUREMENTS ON RING 1

9.1 Observed damage

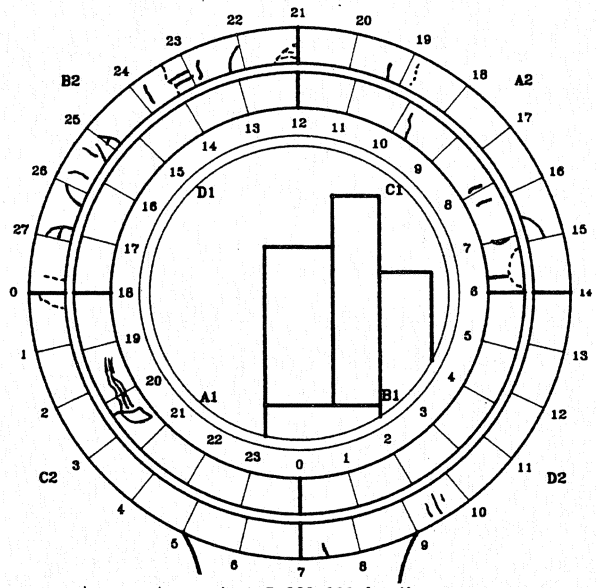


Figure 6 : State of damage observed on ring 1 at 5,000,000 and 1,100,000 loadings and on ring 2 at 500,000 and 2,000,000 loadings.

Figure 6 shows the state of damage observed on the surface of ring 1 at the end of the tests.

At the start of the test, in the first rainy period, a resurgence of clayey fines (pumping) was observed at the joints on the four structures. Drainage from the structure was poor at the beginning of the test ; it was subsequently improved.

Structure A1 :
A gradual cracking of slabs 19-20 and 20-21 began at 750,000 loadings. Other longitudinal cracks appeared in the wheel track, together with a half-moon-shaped crack in each of the slabs, around longitudinal cracks. At the end of the tests, this evolution led to a tight mesh of cracks, with losses of material (photo 3). The end of the tests coincided with a very rainy period, favoring pumping under this damaged slab. Thus, a discharge of treated sand from the subbase was found at the end of the tests at joint 20, on the inside of the ring (low point of superelevation).



Photo 3 : Structure A1 - ring 1 - joint 20. Damage observed at the end of the tests (1,100,000 loadings)

Structure B1 :
A parabolic crack appeared at the edge of slab 5-6, in the first few thousand loadings. It was outside the wheel track, in a zone where the subbase was locally below its specified thickness because of difficulties in levelling the cement-bound sand. This crack continued to grow in slab 5-6 as the total number of loadings increased.

Structure C1 :
A transverse crack went through slab 8-9 at 750,000 loadings. This time, a local weakening of the structure ; the passage of the sleeve for the strain-gauge leads is suspected. The onset of spalling of joint 7 was observed at 850,000 loadings. Another transverse crack appeared in slab 6-7 at the end of the test, at 1.1 million loadings. At the end of the test, these two transverse cracks had not evolved much.

Structure D1 :
No damage was observed on the dowelled structure for the duration of the tests.

9.2 Surface measurements

The surface measurements performed on this first ring confirmed the visual analysis of the behavior of the joints, leading in particular to the decision to resaw in the course of the tests.

They more clearly reveal the extreme sensitivity of the behavior of the slabs to temperature and to temperature gradients.

With the increase of total number of loadings and the wear of the materials, the behavior of the pavement follows a more or less marked course depending on the structure. These differences in evolution are especially well reflected in the measurements made using the LPC collograph. This is illustrated by figure 7, which shows four recordings made by the collograph over the entire duration of the test.

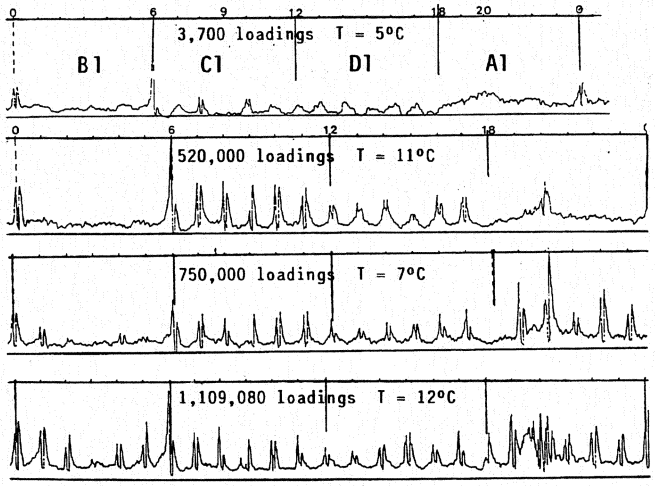


Figure 7 : Surface measurement on ring 1. Evolution of the 4 structures reflected in the collograph recordings.

The first recording, at 37,000 loadings, detected no open joints except for those located at the limits of the structures and joints 8 and 10 of structure C1.

The second recording, at 520,000 loadings, reveals that all the joints of structures C1 and D1 are now open (joint 9 was opened by sawing). A good load transfer is observed on dowelled structure D1. On the other hand, all joints of structures A1

and B1 seem to be closed, except for joint 20. They have not yet been sawn.

The third recording is made at 750,000 loadings, after sawing of the joints of structures B1 and A1. The opening of the sawn joints of structure A1 is clearly apparent. That of the joints of structure B1 is more discreet. In addition, this third collograph recording shows that the behavior of structures C1 and D1 is substantially the same, even though the latter is dowelled.

The last recording of figure 7 was made at the end of the experiment, at 1.1 million loadings. This time, all joints are manifestly open, except for joint 3 of structure B1. Structures C1 and D1 are still very similar in behavior. This collograph recording also detects the damage that appeared on slabs 19-20, 20-21, and 9-10.

10. OBSERVED DAMAGE, SURFACE MEASUREMENTS ON RING 2

10.1 Observed damage

The first stage of the tests was in severe climatic conditions for rigid pavements. Figure 8 shows these test conditions, marked by successions of cold spells with nocturnal frost, rainy weather, or large daily temperature swings. Because of these severe conditions, and in comparison with ring 1, the faultings of the slabs on ring 2 are large, and some are even spectacular. The damage observed at the end of the first stage of the tests on ring 2 is shown in figure 6.

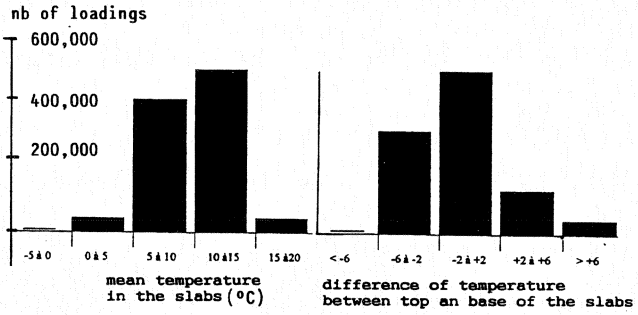


Figure 8 : Climatic conditions during the first stage of the test on ring 2.

So far (August 1992), the main damage observed is on structure B2, which is badly damaged. A very first clear transverse crack was observed on slab 23-24 even before the rotations started. A second transverse crack was found at 250,000 loadings, at 1.1 meter from joint 21 separating structures A2 and B2. At 350,000 loadings, two transverse cracks of the same type were observed on either side of joint 0 between B2 and C2.

The photo 4 shows the common evolution of the three initial transverse cracks. They start from the interior of the slabs perpendicular to the edge, approximately 1 meter from the joint. They then grow, curving towards the joint, which they intersect at 3/4 of its length on the outer side of the ring. Many secondary longitudinal cracks then develop between the joint and the initial parabolic crack.



Photo 4 : Structure A2 - ring 2 - joint 21. Typical evolution of initial transverse crack (view at 500,000 loadings)

The same damage mode is observed thereafter at joints 23, 25, and 26 (800,000 loadings), then 22 and 27 (1.2 million loadings).

The ultimate stage of damage of these regions of meshed cracks is loss of materials when axles pass. Repairs were necessary in the most damaged zones (joints 0, 21, 23, 25, 26) to allow the test to continue.

At the end of the experiment, the appearance of cracking of the foregoing type was also observed on structure A2, towards joints 14 and 19. A rapid evolution of structure A2 is therefore expected to come in stage 2.

10.2 Surface measurements

The measurements made by the LPC collograph are once again given as an example in figure 9. They again illustrate the utility of surface measurements in this experiment.

The first measurement, at 178,000 loadings, shows that the joints of structures A2, B2 and C2 are all open, except for joints 23 and 24 (on either side of the crack before traffic on structure C2) and joint 27. On the

contrary, the joints of structure D2 are barely detected, a sign of its very good behavior.

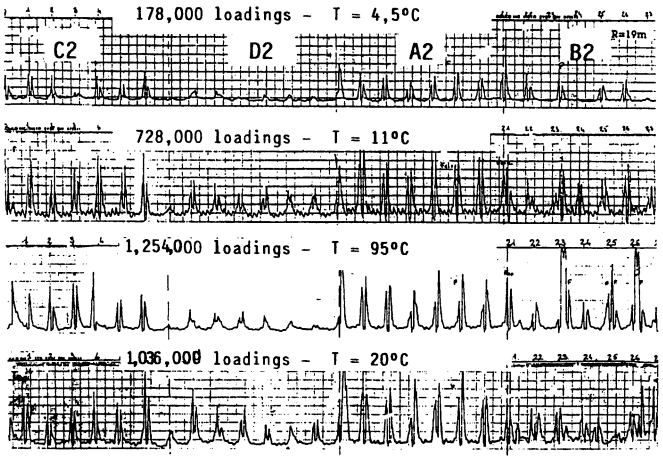


Figure 9 : Surface measurement on ring 2. Evolution of the 4 structures relected in the collograph recordings.

The second measurement, at 728,000 loadings, shows a substantial increase of the movements of the slabs. Dowelled structure D2 continues to exhibit a better behavior than the identical but undowelled structure C2. Joints 23 and 24, on either side of the initial crack of structure B2, are now open, as is joint 27. The collograph signal also shows the advanced state of damage of this structure.

The third measurement, at 1.25 million loadings, confirms the foregoing evolutions. Dowelled structure D2 is clearly differentiated from the three others by its low level of faulting. The advanced damage of structure B2 is slightly indicated, in particular in the zone of the initial crack, whereas the effect of the repairs is perceived in the zone of joint 21.

The last collograph recording, at 2 million loadings, shows an increase of slab movements for all structures. On dowelled structure D2, a substantial impairment of the mechanism of load transfer at the joints was detected. Structure B2, totally destroyed, was repaired to allow normal operation of the circular test track.

On ring 2, there was continuous monitoring of the horizontal opening of joints 7, 1, 19, and 24 (cf. 4.3). The measurement system on joint 24 performs poorly. Figure 10 shows the curves obtained on structures A2, B2, and D2. The curve of variation of mean temperature in the concrete is also shown. The mean opening of the joints is 1.60 mm, 1.20 mm, and 2.20 mm respectively for structures A2, C2, and D2. The daily fluctuations of opening are at most +/- 0.25 mm for the temperature conditions of the test.

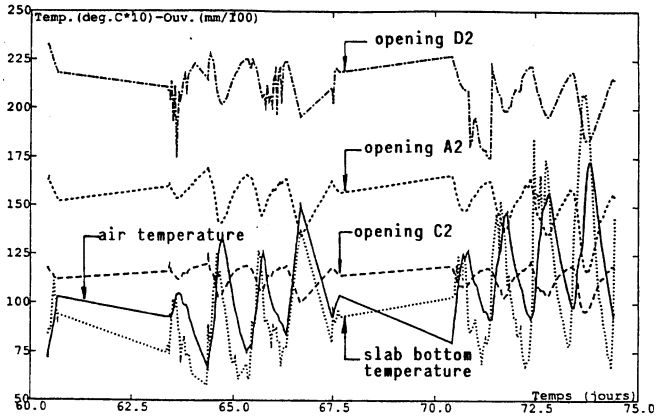


Figure 10 : Horizontal opening of the joints for structures A2, B2 and D2 (mm/100) and temperatures (°C*10) of the air and the bottom of concrete slabs.

11. RESULTS OF STRAIN GAUGE MEASUREMENTS ON BOTH RINGS

11.1 Typical strain-gauge signals, effects of temperature

Acquisition of the measurements on the strain gauges is digital for ring 1 (6). On ring 2, acquisition was analog, because of the very high noise content of the signals, which various digital filtering techniques failed to eliminate on this second ring.

In spite of the low level of the measured strains, rarely greater than 45.10^{-6}, and the high noise level of the signals, 85 % of the recordings made so far have in fact proven to be usable.

Figure 11 shows an example of typical strain-gauge signals obtained on ring 1 for the 4 structures. The recordings presented were made at position P6 of the axle loading (radii 15.50 m), at a speed of rotation of 10 revolutions per minute.

They read the tensile strains in the concrete at the low level, measured respectively by the longitudinal-center (LC), transverse-center (TC), and transverse-upstream joint (TUJ) gauges, for structures A1, B1, C1 and D1. The duration of acquisition of the signals is 1.25 revolution of the fatigue tester, and five consecutive passes of the load are recorded in this way.

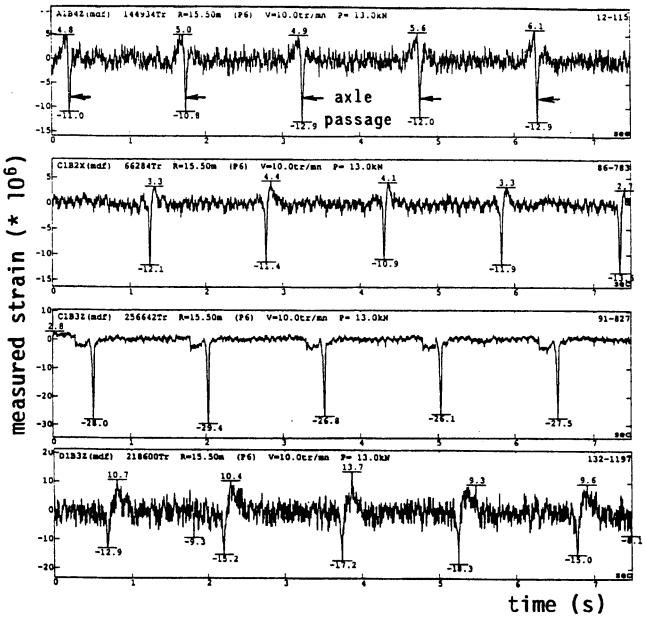


Figure 11 : Typical strain gauge signals obtained on ring 1.

It is clear that the strains indicated by the strain gauges constitute a precious body of data for the development of the numerical model for simulation of concrete pavements, to which this experiment must contribute. The interpretation of these measurements is however made tricky by their large sensitivity to thermal conditions. Figure 12 shows the evolution, during a temperature cycle, of the maximum tensile strains measured under passage of the axles by gauges LC and TUJ of structure A1, at 640,000 loadings. A fluctuation of 11°C of the mean temperature of the slab results in variations of the strains of as much as +/- 25 % of the mean value.

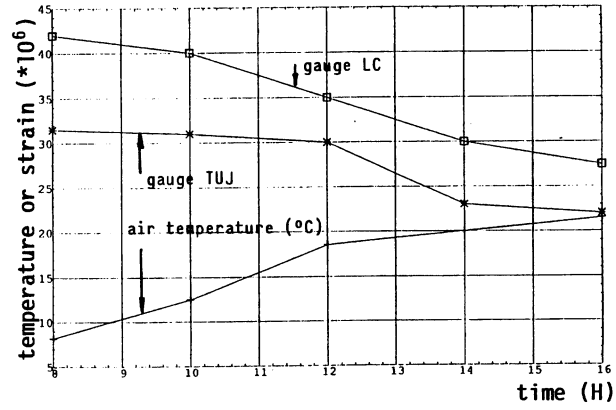


Figure 12 : Evolution during a temperature cycle of the tensile strains measured by gauges LC and TUJ of structure A1.

Systematic examination of the longitudinal and transverse strains measured at mid-height of the slabs leads to low values, always less than 5.10-6. Thus, the eight structures in fact confirm the hypothesis of perfect sliding contact of the concrete on its subbase, used in the routine design of these structures.

11.2 First results, center-joint comparisons

The work of analysis and interpretation of these measurements is currently in progress, and the experiment has not yet reached the assigned number of loadings. But some tendencies can already be discerned in the first results analyzed.

Figure 13 provides a direct comparison, for the four structures of ring 2 and all usable measurements of the longitudinal and transverse strains at the center of the slab (gauges LC and LT). In spite of the dispersion of these measurements, a preponderance of longitudinal strains over transverse, in a ratio ranging from 1 to 2.8, is apparent in this presentation.

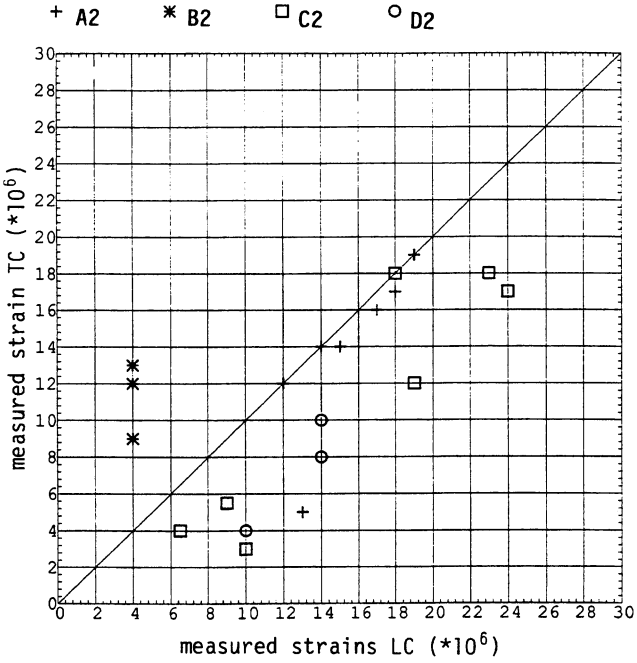


Figure 13 : Comparison of the longitudinal strains (LC) with the transverse strains (TC) at the center of the slabs.

These results are in concordance with the theoretical results of the Alizé semi-infinite multi-layer elastic model (4) used in France. This model in fact indicates a ratio of 1.7 to 2 depending on the structure.

Figure 14 uses the same presentation to compare the longitudinal strains in the center of the slab (TC) with the transverse strains at the upstream joint (TUJ). A preponderance of joint transverse strains is observed for ring 1 (ratio

TUJ/TC between 1.2 and 2.5, not shown on the figure). On the contrary, the measurements on ring 2, while more scattered, show a preponderance of transverse strains at the upstream joint, mainly for the structures B2 and C2.

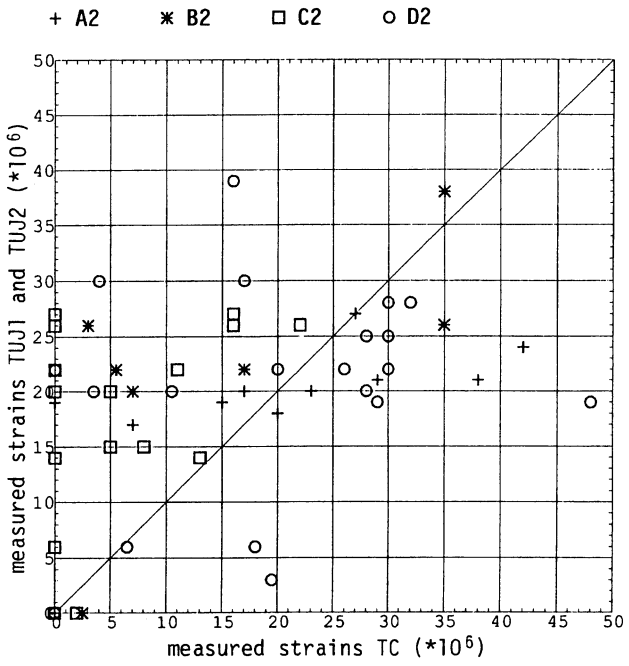


Figure 14 : Comparison of the transverses strains in the center of the slabs (TC) with the transverse strains at the upstream joint (TUJ).

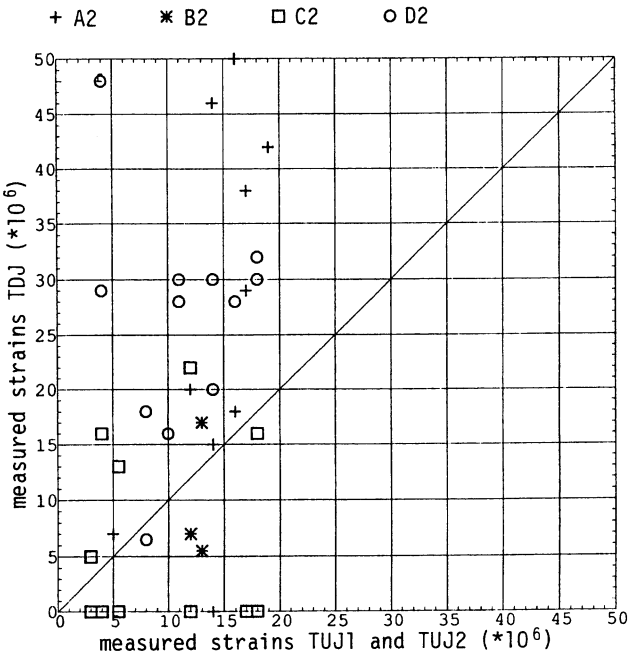


Figure 15 : Comparison of the transverse strains at the upstream joints (TUJ) and the strains at the downstream joint (TDJ).

The comparison of the transverse strains at the upstream joint (TUJ) and downstream joint (TDJ) at the low level in the concrete is given by figure 15 (ring 2). A lower level of strain downstream generally emerges from these results, except for the measurements on structure B2. A lower level of strain downstream is observed for this structure, as for structure B1.

11.3 The effect of dowels

It is tempting to try to assess the effectiveness of dowelling of the slabs by comparing the strains measured in identical structures C and D (figure 16). A slight tendency towards the preponderance of longitudinal strains at the center (LC) is noted in dowelled structures D1 and D2 (not shown on the figure). The tests on rings 1 and 2 disagree concerning the transverse strains at the upstream joint (TUJ). On ring 1, the dowelling of structure D1 is reflected by a reduction of the transverse strains at the joint by 0.65 to 0.84 with respect to structure C1.

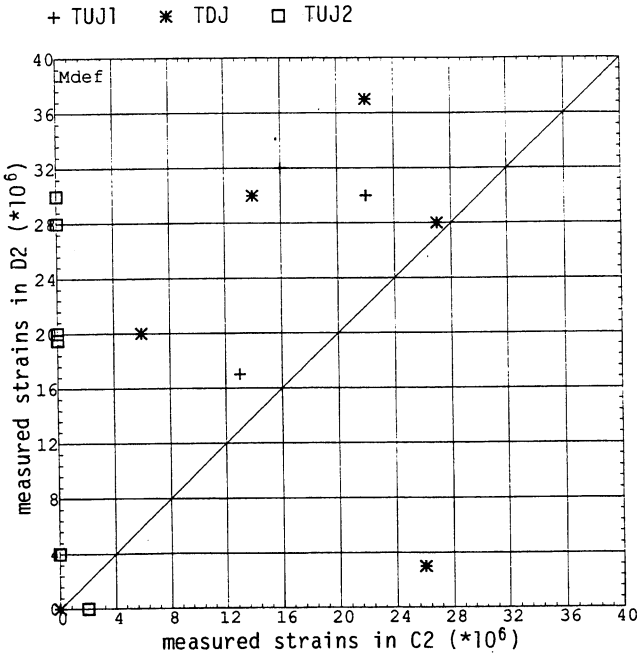


Figure 16 : Effectiveness of dowelling. Comparison of the strains measured in the structures C2 and D2 for transverse strains at joints.

On ring 2, the dowelling is reflected by an increase of these strains that defies logic, in ratios of 1.1 to 2.

An example of the shear and bending strains recorded in a dowel of structure D1 is given in figure 17. On both structures D1 and D2, one notes a substantial increase of the bending

strains in the dowels with the number of passes of axles.

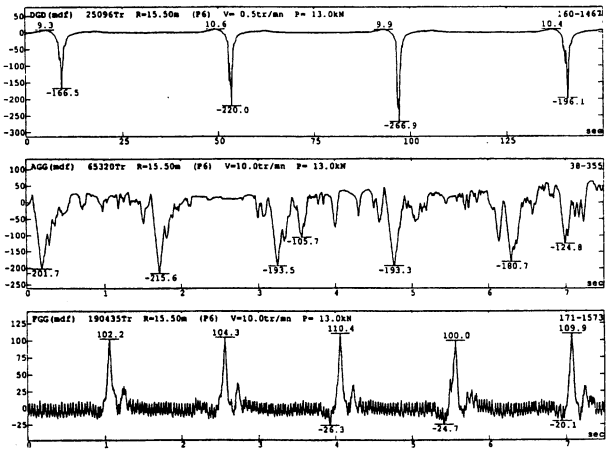


Figure 17 : Typical signals of the strain gauges on dowels obtained on structure C1, ring 1.

The distribution of the shear forces among the dowels of a given joint is shown in figure 18 : at 230,000 loadings for structure D1-joints 14 and 16, and at 125,000 loadings for structure D2-joints 9 and 12. A good diffusion of the forces between the dowels of a joint is attained in structure D1 (diameters of the dowels: 32mm). On the contrary, the taking out of the forces is strongly concentrated on the dowels located under the load for structure D2, using dowels of smaller diameter (22 mm).

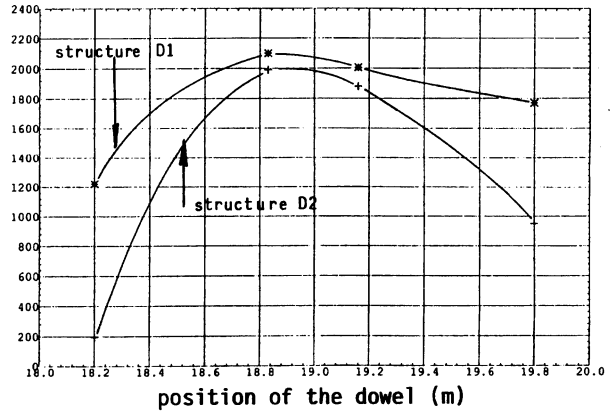


Figure 18 : Distribution of shear forces among the dowels of a joint. Measurement on structure D1.

The analysis of the strain-gauge signals has not yet been completed, and their acquisition will continue with the loadings still to be performed. Accordingly, the presentation of the gauge measurements will be limited in this article to the main current elements provided above.

12. THEORETICAL MODELLING : FIRST CALCULATIONS

12.1 The fem code César-LCPC

A large part of this experiment on the fatigue test track is devoted to the theoretical interpretation of the measurements. In addition to the adjustment of the present Burmister's multi-layer model of the catalogue, this study is aimed at the development of a numerical model capable of more realistically simulating the modes of functioning of concrete structures. The finite-element calculation method was chosen for this work; we are unaware of any other theoretical model capable of reproducing, with sufficient accuracy, the behavior of these discontinuous structures (7).

The calculation code used is the César-LCPC software package (8). The calculation code is the product of theoretical and numerical research work done by the LCPC for about twenty years. It is intended for solving the most varied geomechanical and civil engineering problems and its main capabilities include:

- 2D and 3D calculations ;
- treatment of static or dynamic mechanical problems, and thermal, hydraulic, and diffusion problems ;
- linear and nonlinear elastic and visco-elasto-plastic constitutive laws ;
- interface laws with friction and separation criteria ;
- crack propagation model (2D) ;
- graphic coprocessors for interactive data entry and for the processing and display of results ;
- ability to run on Unix workstations.

12.2 Modelization of the structures of ring 2. First results

Figure 19 shows the slab displacements yielded by César-LCPC for structure C2, axle tangential to the joint, on the assumption of completely open joints (no load transfer). The mesh corresponding to lean concrete and foundation is not shown.

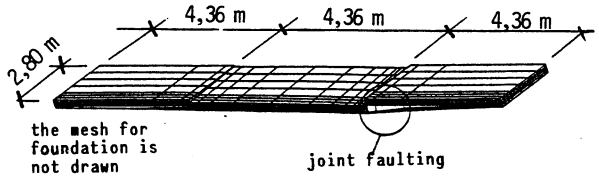


Figure 19 : Theorical modelling with Cesar-LCPC. Calculated slabs displacements of structure C2.

The calculations are necessarily performed in three dimensions. The mesh consists of hexahedral isoparametric elements with 20 nodes. The axle (65 kN on 2 wheels) effect is represented by a static load of constant pressure applied to a double imprint (20 xm x 30 cm, 30 cm inter-axes, 0.542 MPa vertical pressure.

The faulting is visible. It is initiated by the installation of contact elements having a separation criterion at the surfacing between the concrete-lean and concrete interface.

The subbase is represented by a continuum having an elastic behavior. In spite of its great numerical advantages, Winkler's model is not used, because of a lack of representativeness and difficulties in determining the notorious (or all-important ?) soil reaction modulus.

For the interpretation of fatigue track tests on concrete, this complete calculation code needs further development in only one direction: for the modelling of load transfer mechanisms between slabs, with and without dowels. This work is now being done (August 1992).

The installation at between-slab interfaces of contact elements having a friction criterion (Mohr-Coulomb) was tested. It increases memory requirements excessively, and in 3D raises convergence difficulties. The individual representation of dowels poses the same memory problems.

The physically very complex phenomenon of load transfer between slabs must absolutely be reduced to a numerically simple mechanism, despite the current power of the fem.

The simple joint elements linking facing points of adjacent slabs currently used in the calculations are of two types. As appropriate, they ensure :

- the continuity of vertical displacements on either side of the joint (perfect hinge-joint) or a linear relation between these two displacements (hinge-joint with known vertical play) ;
- a linear relation of rigidity Kx, Ky, Kz between the differential displacements vector and the force vector.

Figure 20 shows the strains calculated by César-LCPC at the base of the four structures A2, B2, C2 and D2 for slab center and edge of joint load positions. For load at center, the most severe tensile stresses are the transverse strains at the center, in agreement with the experimental results (figure 14).

The dowelling of structure D2 is reflected in a reduction by about 8 % of the transverse stresses at the edge. This tendency is in good agreement with the measurements made on structures C1 and D1. The opposite effect measured on structures C2 and D2 remains, of course, unexplained.

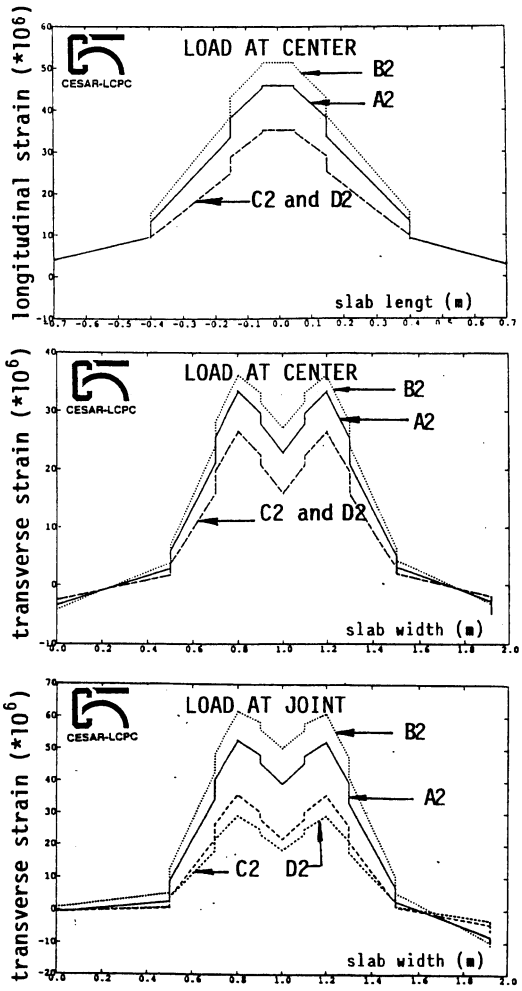


Figure 20 : Theorical modelling with Cesar-LCPC. Strains calculated at the base of the structure for positions of load at slab center and edge of joint.

13. CONCLUSIONS

The current conclusions of the experiment are provisional, pending the last stage of testing on ring 2.

It is already clear that the LCPC fatigue test track is a very useful tool for experiments on rigid structures. The tests have permitted to accurately reproduce the modes of functionning and damaging of actual concrete structures.

In the first analysis, the behaviour of the two rings is very similar to that

described by the dimensioning method : practically no breaking on ring one ($1.1.10^6$ loadings and 80 % risk of breaking), nor on ring two after 2.10^6 loadings, except on structures with no foundation. Their behaviour seems to confirm the current limits of the dimensioning method : the extent of erosion resistance in the base layer, even when a pervious geotextile was used (ring one) and probably poor estimation of the conventional properties of the lean concrete used in the calculation method (ring two).

The finite-element method provides a model that can reproduce the complex functioning of concrete structures realistically enough to be useful. However, the importance of thermal, hydraulic, and hygral phenomena in damage to concrete structures is manifest. It is still difficult to imagine a global rational mechanical model incorporating these many factors.

ACKNOWLEDGEMENT

Grateful acknowledgement is made to Christophe GAUDIN, graduate student, Saint Nazaire University Institute of Technology, for his active contribution to the analysis of the experimental results.

The authors also express their satisfaction with the quality of the cooperation between French Highway Department and National Association of Concrete Pavement Contracting and cement Industries, a big factor in the succes of this experiment.

REFERENCES

1. LCPC, SETRA, *"Le Catalogue des Structures Types de Chaussées Neuves, actualisation 1988"*, LCPC- SETRA, Direction des Routes, Paris, 1988.

2. P. Autret, A.-B. de Boissoudy, J.-C. Gramsammer, *"The circular test track of the Laboratoire Central des Ponts et Chaussées- Fisrt results"*, Proc. 6th Int. Conf. on Structural Design of Asphalt Pavements, Ann Arbor, Michigan, 1987, pp. 550-561.

3. G. Caroff, J.-L. Nissoux, F. Vehree, *"Structural design of concrete pavements"*, 5th. Int. Symposium on Concrete Roads, Aachen, 2-4 june 1986, pp.13-26.

4. P. Autret, A.-B. de Boissoudy, J.-P. Marchand, *"Alizé 3 practice"*, Proc. 5th Int. Conf. on Structural Design of Asphalt Pavements, Ann Arbor, Michigan, 1982, pp. 174-191.

5. J.-C. Gramsammer, J.-P. Poilane, M. Louet, J.-P. Nerfie, *"Le collographe,* Bull. liaison Labo. P. et Ch., 126, juil.-août 1983, Réf.2821, pp. 77-90.

6. J.-G. Gramsammer, J.-P. Kerzreho, *"Data acquisition system for the circular test track of the LCPC"*, proc. Colloque Route et Informatique, Paris, 13,15 march 1990, Presses de l'école nationale des Ponts et Chaussées, Paris, pp. 1007-1024.

7. PIARC Committee on Concrete Road and CEMBUREAU, *2nd Int. Workshop on the Theorical Design of Concrete Pavements*, 4-5 oct. 1990, Sigüenza, Spain, 621 p.

8. P. Humbert, *"César-LCPC, un code général de calcul par éléments finis"*, Bull. liaison Labo. P. et Ch., 160, févr.- mars 1989, Réf.3389, pp. 112-115.